SAE AERODESIGN WEST

"THE WRIGHT STUFF"

By
AARON LOSTUTTER, ADAM NELESSEN, JACOB VINCENT, ZEV VALLANCE, AND BRANDON PEREZ
Team 10

FINAL REPORT

Document

Submitted towards partial fulfillment of the requirements for
Mechanical Engineering Design – Spring 2013

Department of Mechanical Engineering
Northern Arizona University
Flagstaff, AZ 86011

Contents

List of Figures

List of Tables

Acronyms and Symbols

μ_r	Coefficient of rolling friction
$\delta_{A\max}$	Aileron deflection
ρ_∞	Ambient air density
ABS	Acrylonitrile Butadiene Styrene
AR	Aspect Ratio
C_a	Aileron chord
b_a	span
c	Wing chord
C_D	3D Polar Drag
$C_{D_{min}}$	Summation of the pressure and skin friction drag contributions from all airplane components
C_f	Skin friction coefficient
CG	Center of Gravity
C_L	Coefficient of lift
$C_{L_{min}}$	Minimum coefficient of lift
$C_{L_{max}}$	Maximum lift coefficient
CNC	Computerized Numeral Controlled
D	Total aircraft drag
e	Wingspan efficiency
FDM	Fused Deposition Modeling
FF	Form Factor
g	force of gravity
K'	Inviscid induced drag factor
K''	Viscous induced drag factor
L	lift required for takeoff.
NACA	National Advisory Committee for Aeronautics
R/C	Radio Controlled
RPM	Rotations per Minute
S_1	Maximum control surface deflection
S_2	Maximum Servo Deflection
S	Wing planform area
S_a	Aileron planform
S1223	Selig 1223 Airfoil
s_{LO}	Liftoff distance
$S_{planform}$	Planform area of the components
S_{wetted}	Wetted surface area
T	Thrust
V	Velocity
V_H	Tail volume ratio
l_H	Horizontal stabilizer moment arm
S_H	Horizontal stabilizer planform area
W	Aircraft weight

1. INTRODUCTION

This document describes the final design produced by the Wright Stuff of Northern Arizona University (NAU) for participation in the Society of Automotive Engineers (SAE) Aero Design West 2013 competition. SAE competitions provide an opportunity for student teams to gain real world engineering experience through collaborative design. In this particular event, the design objective is to develop a remote-controlled aircraft to takeoff, maneuver, and land predictably while carrying as much payload as possible. Along the way, students learn important lessons in aerodynamic and structural design, team organization, time management, cost and budgeting, and manufacturing. Through innovative system design, the Wright Stuff has designed and built an aircraft that successfully met the mission requirements in April 2013.

1.1. OBJECTIVE

The objective of the Wright Stuff was to introduce precision manufacturing techniques to the development of a remote-controlled aircraft in order to optimize its aerodynamic performance and payload capacity.

1.2. REQUIREMENTS AND SPECIFICATIONS

The following is a list of fundamental requirements that have been observed by the design team throughout the planning and production of the final design.

Table 1: Competition requirements

R1	Aircraft must lift from the ground within a take-off distance of 200 feet
R2	Aircraft must remain intact during takeoff and landing
R3	Aircraft must successfully complete one 360 degree circuit of the field
R4	Aircraft must touch down and land within 400 feet
R5	Aircraft must be controllable in flight
R6	Aircraft shall not exceed a combined length, width and height of 225 inches
R7	Aircraft may not weigh more than 65 pounds with payload and fuel
R8	Aircraft must provide capability of securing and unloading payload in less than 1 minute
R9	Aircraft components may not consist of any Fiber-Reinforced Plastic or lead

2. DESIGN PROCESS

2.1. DESIGN PHILOSOPHY

The philosophy of this team throughout the design process has centered on developing sound fundamental concepts to satisfy competition requirements. Therefore, the focal point for the team was to create an airplane that performs well in several critical areas, which will hereafter be referred to as objectives. Table 2 displays these team objectives.

Table 2: Team objectives

O1	Generate sufficient lift
O2	Minimize drag effects
O3	Maintain longitudinal and vertical static stability
O4	Provide adequate maneuverability
O5	Achieve the necessary structural strength
O6	Minimize overall weight
O7	Takeoff and land within distance constraints

The team identified additive manufacturing as an important means to fabricating an airplane that will satisfy the stated objectives and perform well in flight. The ability to 3D print airplane features will be utilized in this project to fabricate the aerodynamic surfaces of the wing to a high level of precision.

2.2. RESEARCH

Before construction began, conceptual design process was used to outline the various design options, weigh the advantages and disadvantages of each, and decide on the best choice. Physical tests were performed in order to select the optimum propeller and to measure the airplane's center of gravity following the construction of the first prototype. Finally, a flight test was conducted on the second prototype in order to evaluate proper function of the entire system and aircraft maneuverability. The following sections describe these steps in detail.

2.2.1. Conceptual Design

The teams design process was performed one component at a time, in an effort to guarantee a high performance level for each element of the system. In each section, the relevant team objective is noted, the various options are presented and analyzed, and the outcome of the conceptual design process is reported.

Airfoil Selection

Selection of an airfoil for the wings is the primary means to satisfying team objectives O1 and O2. For a small cargo plane application such as this one, the wings must provide high lift at an approximate Reynolds number of 200,000. This Reynolds number was calculated using an assumed aircraft velocity of 55 ft/s, a chord length of 1 ft and historical environmental conditions [1]. Examination of previous NAU team documentation showed that the Eppler 423 has performed well in the past. In order to improve upon previous results, however, the team investigated other airfoils such as the S1223, which was not used by NAU teams before because it is very difficult to cut out of balsa.

Lift and drag coefficients for each airfoil were determined using XFOIL [2] at a Reynolds number of 200,000. The left side of Figure 1 shows plots of lift coefficients of these airfoils as a function of angle of attack. Lift to drag ratios for the airfoils were also determined, and are plotted on the right side of Figure 1.

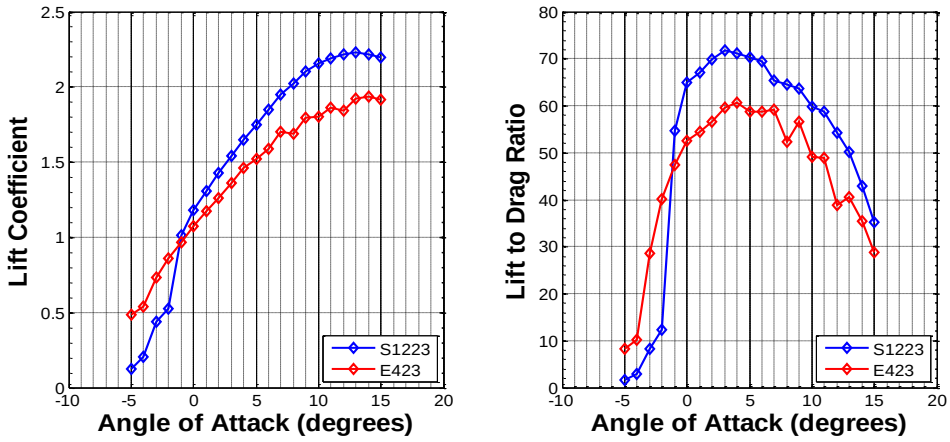

Figure 1: Lift coefficient vs. angle of attack (Left) and lift to drag ratio vs. angle of attack (Right)

Data from Figure 1 show that the S1223 airfoil will provide 10-20% more lift than E423 airfoil within the practical angle of attack range. In addition, the lift-to-drag ratio is as much as 18% higher for the S1223 than the E423 within the practical angle of attack range. The ability to employ additive manufacturing techniques, as described below under Innovations, will give this team's entry exceptional aerodynamic performance via selection of the S1223 airfoil.

Wing Planform

The planform of a wing, or its top down planar area, contributes significantly to its aerodynamic performance, particularly in terms of 3D drag due to wingtip vortex shedding. Thus, the selection of the best planform will allow the team to satisfy objective O2. The different planforms considered were square, elliptical, and tapered, as shown in Figure 2.

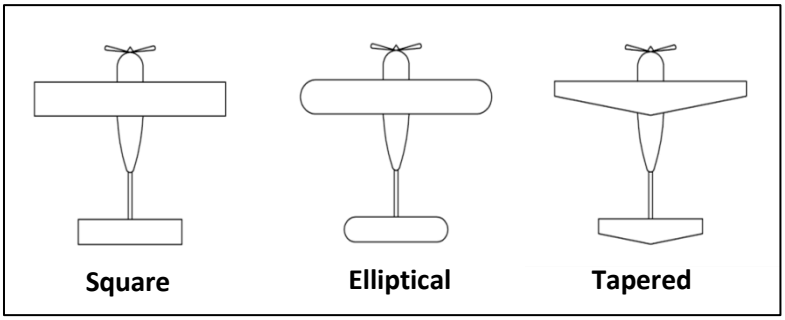

Figure 2: Wing planform options

In terms of aerodynamic performance, the elliptical wing allows for the greatest drag mitigation, followed by the tapered planform [3]. However, these designs are more difficult to manufacture than the square planform. After weighing these advantages and disadvantages, the team decided to pursue a wing planform that included elements of both the square and elliptical options. The majority of the wings are square, with a constant chord and spars of uniform outer diameter. However the tips of the wings have been capped with Hoerner wingtip extensions, which have an elliptical curvature when viewed top-down, for wingtip vortex reduction [4]. The effective result of this concept is a wing that is easily and precisely manufactured, yet also performs well in terms of 3D drag mitigation.

Wing Configuration

Configuration design for the wing was focused on the location of the wing relative to the fuselage. This concept has an influence on the ability of the team to accomplish objectives O3 and O6. The mid and high locations, as shown in Figure 3, were considered for mounting the wing whereas the low location was neglected due to its dangerous ground clearance and reduced head wind velocities.

The notable advantage of mounting the wing in the middle of the fuselage is that weight may be saved by integrating the structural parts of the wing into the structure of the fuselage itself. However, this wing location may take up space in the fuselage that may be needed for housing of the payload or other components.

Placing the wing above the fuselage, on the other hand, is advantageous because it leaves the fuselage open for payload and component housing. This configuration would allow the team to locate the payload near to the center of gravity of the entire airplane, which is very advantageous from a longitudinal stability perspective. Additionally, the high placement of the wing allows the wing to be easily removable, which simplifies the vehicle transportation process to competition or flight test locations.

In the design process, a center of gravity that varies minimally with the addition of payload was considered to be of high value to the team. Thus, the high wing configuration was selected.

Tail Configuration

The fulfillment of objective O3 requires the addition of two primary stabilizing components, the horizontal and vertical stabilizers. The horizontal stabilizer provides longitudinal stability in pitch, which is a rotation that moves the nose up or down. The vertical stabilizer provides stability in yaw, which is a rotation that moves the nose left or right. Airplane rotational degrees of freedom are shown on the left side of Figure 3 and a general tail consisting of a vertical and horizontal stabilizer is shown on the right side of Figure 3.

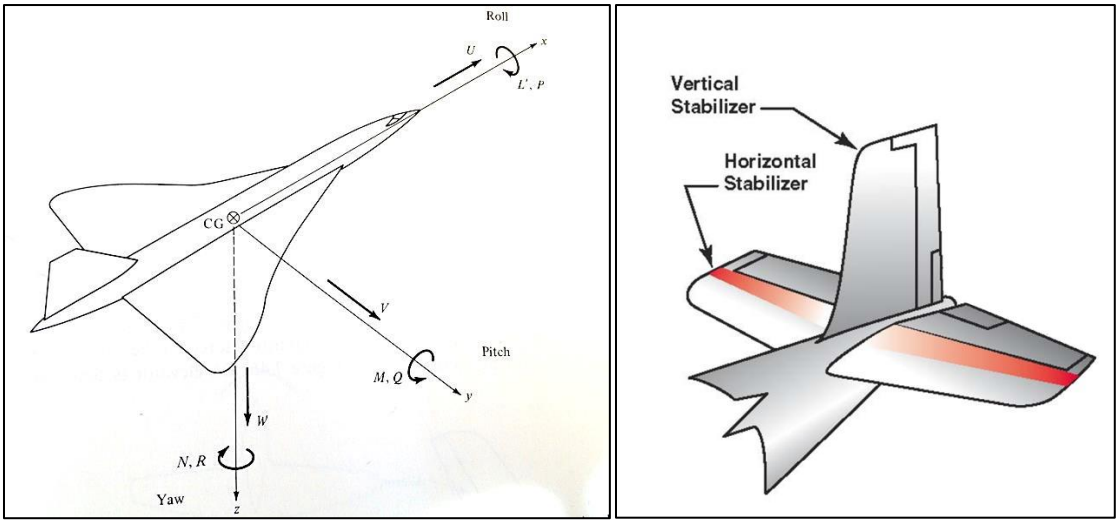

Figure 3: Aircraft rotational degrees of freedom (left) [5] and a typical airplane tail (right) [6]

The team considered different types of stabilizer configurations, such as surfaces made from symmetrical airfoils, cambered airfoils, and flat plates. Symmetrical airfoils provide exceptional drag reduction and moderate amounts of lift, but can be somewhat heavy as a consequence of their relative thickness. Cambered airfoils offer more lift, at a cost of even more drag and weight. Finally, flat plates offer relatively low drag and weight, but do not contribute much lift [3]. Ultimately, the team decided that lift contributions from stabilizing surfaces are not necessary. This suggested that the lightest stabilizers possible should be used, since the main wing is designed to provide the bulk of the lift

generated by the aircraft. Consequently, flat plates with chords that taper down with distance from the fuselage were selected in order to support fulfillment of objectives O2, O3, and O6.

Control Surfaces

The SAE requirement of maintaining maneuverability and control of the aircraft during flight, identified as objective O4, necessitates the inclusion of several control surfaces. The motions that must be controlled are the rolling, yawing, and pitching motions of the airplane. These motions were shown in the previous section as Figure 4. Ailerons were implemented to control the rolling motion, a rudder to control the yawing motion, and an elevator to control the pitch motion. A generalized aircraft pictured in Figure 4 shows these control surfaces and the effects they can have on the orientation of an airplane is seen in Figure 4.

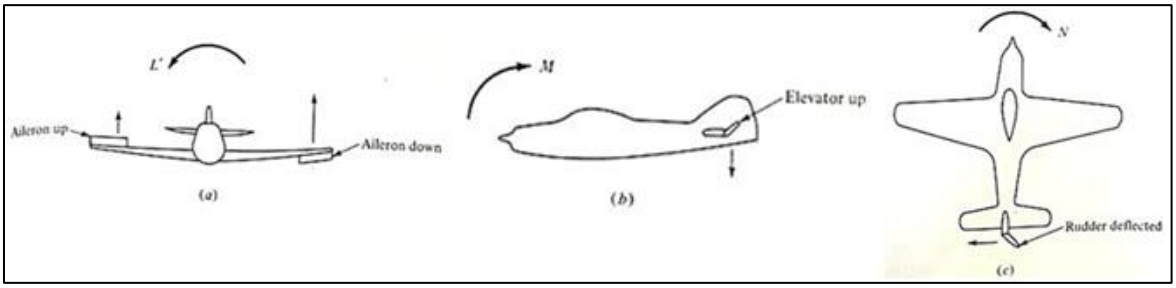

Figure 4: Control surfaces and their effects on airplane orientation [5]

The decision to add these features is a result of a comprehensive review of modern cargo airplane theory, and our school's previous entries to this competition [4]. Control surfaces will be actuated by servos of varying sizes and supplied torques. These surfaces will mimic the shapes of the wing and tail as much as possible. They will be constructed primarily out of balsa and supplemented with small manufactured components as necessary to mimic the taper of the wing trailing edge.

Fuselage

The fuselage is the backbone of an airplane; it serves as a connecting piece for the engine, wing, and tail as well as housing for payload and other components. This body is a geometrically large piece of the total system and will experience significant loading during landing. Thus, there are many weight,

aerodynamic, and structural considerations that must be addressed in the design of a fuselage. Its length is a very influential factor in the stability of the airplane as well. In summation, the fuselage must be designed properly in order to successfully meet objectives O2, O3, O5, and O6.

From an aerodynamic perspective, it is important that the body is streamlined so that air is able to flow around it in such a way that keeps drag effects low. As mentioned before, symmetrical airfoils are typically very drag-efficient shapes. The team made it a priority, therefore, to design the fuselage to approximate the shape of a symmetrical airfoil. Figure 5 shows a computer aided sketch of the fuselage viewed top-down. Overlaid on this sketch, the NACA 0012 airfoil is plotted for comparison. Figure 6 shows that the overall shape of the fuselage closely matches the symmetrical NACA 0012 airfoil. This streamlined body shape will keep drag effects of the fuselage to a minimum.

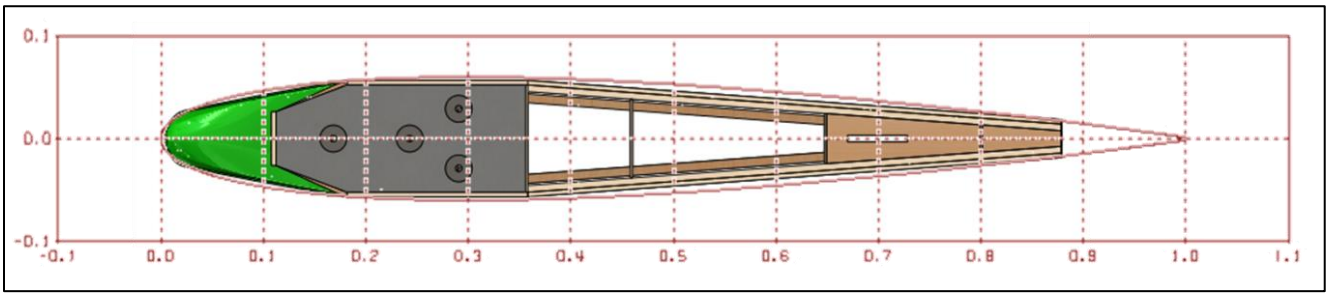

Figure 5: Fuselage comparison to NACA 0012 airfoil

The dimensions of the fuselage were designed such that the tail can be considerably reduced in size, yet still provide the necessary stabilizing effect. By locating the tail at a greater distance from the center of mass for the aircraft, the pitching moment provided by the tail is increased without the need for a larger control surface. The effect of this design will be to keep weight low and enhance aircraft stability.

Once the aerodynamic and stability considerations had been addressed, the fuselage was constructed. It was manufactured to be lightweight yet strong by selecting a commercial-grade panel of aluminum honeycomb as the backbone. The wings, payload, and wood structural materials are all affixed to this panel. Balsa stringers reinforced with basswood bulkheads add torsional and bending

strength to the fuselage as well as mounting locations for the engine and electronics. Finally, wooden dowels made of basswood are used in a truss configuration to give the fuselage extra compressive strength in bending due to landing forces. Wooden materials were used whenever possible to mitigate unnecessary weight aft of the intended center of gravity.

Landing Gear

In order to fulfill objective O7, it was essential to design and construct landing gear that would allow the plane to take off and land successfully. Another important function of the landing gear is to absorb the impact of landing so that more rigid parts of the airplane aren't damaged by the dynamic loads. The team considered two different landing gear configurations in the design process: the taildragger and the tricycle. These are shown in Figure 6.

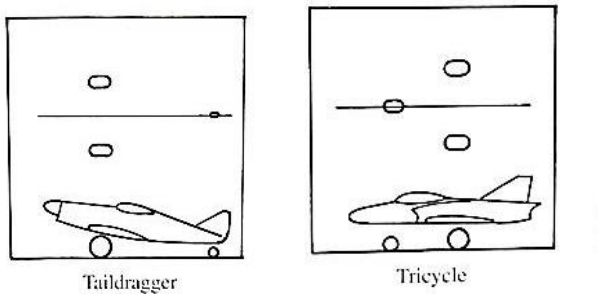

Figure 6: Landing gear options [4]

The taildragger landing gear configuration consists of two large wheels below the wings and a small wheel below the tail. This results in increased angle of attack while the airplane is rolling on the ground, which increases the lift generated by the wings. In addition, the taildragger gear gives more propeller clearance and weighs less than the tricycle landing gear [4]. The major disadvantage of using a taildragger gear is that it can be unstable and therefore difficult to land due to its embedded angle of attack. The tricycle gear, on the other hand, is more stable in landing but because the third wheel is larger in this configuration, this option is heavier. The team selected the taildragger because it is expected that the final aircraft will be stable and controllable, thus making the landing process more

predictable. The increased lift and propeller clearance were important motivating factors in making this decision.

Propeller

Propellers are mechanisms which generate thrust from rotary motion. This thrust enables the generation of lift by providing relative motion between the wings and the air. Thus, the selection of the best possible propeller is essential for the fulfillment of objective O1. When selecting a propeller, the important variables to consider are diameter and pitch. The practical RPM range and the displacement of the selected engine dictate that the propeller diameter range should be between 11 and 14 inches. The final propeller selection was made based on results from a static thrust test, which is described below in the Static Thrust section.

2.2.2. Physical Testing

After the completion of the conceptual design process, several physical tests were performed to ensure that real systems and subsystems performed as intended. Data acquired from these tests prompted several changes, leading to two successive design iterations before a final design was reached. These physical tests are described in the subsequent sections. Included in the discussion for each test are lessons learned and the effects they had on later design iterations.

Static Thrust Testing

Static thrust testing was performed by the team in order to select the optimum propeller for the design objective. This test was performed in Phoenix, Arizona because of its similar air density to that of the competition location of Van Nuys, California. A static thrust testing stand was constructed out of lumber, a rotating pin connection, an engine mount, and a digital scale. As the engine is displaced by the thrust of the propeller, its rotation causes a force to be imparted to the plate of the digital scale by trigonometry. This experimental apparatus is shown in Figure 7.

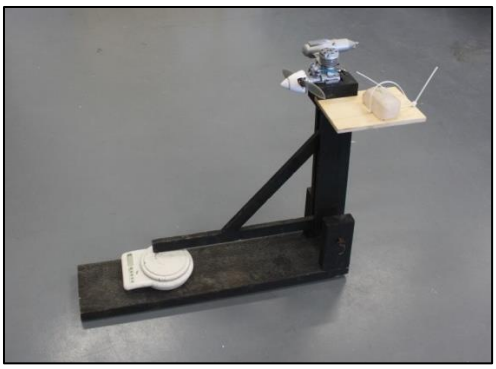

Figure 7: Static thrust experimental apparatus

The apparatus outputs a force measurement, which is assumed to be a conservative estimate of the static thrust provided by the propellers, because the frictional effects of the device are likely to lower the force values output by the scale. Four propellers were examined in this test. The propeller specifications, engine RPM values at which the maximum thrust was produced, and maximum thrust produced by each are shown in Table 3.

Table 3: Static thrust testing results

Propeller	RPM	Thrust (lb)
11X7	11,400	5.51
12X7	10,000	5.22
13X4	10,500	7.28
14X4	9,300	8.16

Table 3 shows that the maximum thrust occurs with the use of the 14X4 propeller, which is the expected result. It is worth noting that during testing, the operators of this apparatus observed a significant amount of engine strain when the 14X4 propeller was attached. This effect was influential in propeller selection, as the first two prototypes included the 13X4 propeller. Following the learning experiences of the flight test, as discussed below in the Flight Testing section, the 14x4 propeller would eventually be selected for the final design.

Center of Gravity Testing

In order to determine the location of the aircraft center of gravity (CG), which must be placed properly to achieve longitudinal static stability [5], a simple device for taking airplane balance

measurements was assembled and utilized. This device consists of a vice which firmly clamps down on two wooden dowels, which are taped on the ends to add friction. Figure 8 shows this center of gravity testing stand in operation.

Figure 8: Center of gravity testing

The first time this test was performed took place after the construction of the first airplane prototype. This prompted a series of major adjustments, as the CG was found to lie several inches aft of the proper location, which would make the airplane tail-heavy and inherently unstable. Thus, the second prototype included a tail that was a tenth of the weight of the original, and mounted 4 inches forward. Also added was a set of 2 inch engine mount extensions to increase the static moment forward of the center of gravity. The result was a suitable unloaded CG location of roughly 22% of the wing's mean aerodynamic chord. In formulating the final design, the CG location would later be fine-tuned as needed to achieve longitudinal stability. The supporting calculations for this process are shown below in the Stability and Control section.

Flight Testing

First Flight Test

One of the most influential steps of the design process was the first flight test. In early March, the team met with several members of the Flagstaff Flyers, a group of local remote-controlled aircraft enthusiasts. After consulting with the pilot, making some last-minute adjustments, and programming

the transmitter, the airplane was ready for takeoff. Figure 9 below shows a time-series of photographs of the plane during this brief flight of the 2nd prototype.

Figure 9: Flight test time-series

The aircraft suffered a crash-landing moments after takeoff. The time-series of Figure 10 shows severe positive pitching and rolling motions that occurred almost immediately after the plane left the ground. Following this flight test, the team discussed possible design failures with the pilot and other Flagstaff Flyers. Upon reviewing the flight tape and lessons learned in this process, several adjustments were made to the final design of the aircraft:

- Wing angle of attack was made to be adjustable
- Horizontal stabilizer angle of attack was made to be adjustable
- Horizontal stabilizer wing planform was increased by 50%
- Propeller size was increased
- CG was shifted forward by 10% of the wing mean aerodynamic chord
- Wing dihedral angle was increased from 0° to 3°

The flight test yielded a significant amount of usable data. It was found that the large angle of attack in the wings that caused the drastic lift. Thus, this stalling tendency was corrected by decreasing that angle of attack by simply adding adjustability to the wings by adding shims to the mounting assembly. In addition, the horizontal stabilizer was increased in size to enhance the stability of the aircraft. Furthermore, dihedral will add to the lateral stability of the aircraft [4].

Second Flight Test

After the design changes described above were implemented and a new prototype was completed, the team validated these changes with further flight testing. This time, the aircraft was taken to Leupp, Arizona, where the elevation is closer to that of the competition location and a large, clear space was available. This allowed the team to test the aircraft's ability to takeoff and maneuver with various levels of payload while also lowering the risk of a catastrophic crash. In these tests, the airplane successfully flew and landed five times with various amounts of payload ranging from 0 to 10.5 pounds. This flight test demonstrated that the design was ready for competition.

2.3. FINAL DESIGN

The final design is the result of extensive conceptual design, engineering analysis, and physical testing. A detailed plan for this design is attached to this document as Appendix A.

Wing

This design includes a square wing capped with an elliptical Hoerner wingtip, bent to a dihedral angle of 3° and a sweep angle of 1° after the middle spar. The front and rear spars are 6 foot long hollow aluminum tubes, extended with matched-diameter wooden dowels. A short, hollow aluminum spar is included in the middle to fortify the wing where maximum bending occurs. Wing ribs are constructed of acrylonitrile butadiene styrene (ABS) by a Dimension 768 SST, fused deposition modeling (FDM) system into the shape of a constant-chord S1223 airfoil.

Tail

The tail consists of a curved-planform vertical stabilizer and a tapered-planform trapezoidal horizontal stabilizer. The vertical stabilizer thickness tapers from leading edge to trailing edge. The horizontal stabilizer is a constant-thickness flat plate with a rounded leading edge.

Control Surfaces

Separate ailerons are installed on each wing to provide roll control. These are 20% of the wingspan in length, and are built with ABS ribs and reinforced by thin balsa stringers to achieve the same airfoil cross-section in the neutral position. A flat-plate elevator with a sharp point on the trailing edge is installed aft of the horizontal stabilizer to provide pitch control. A curved rudder is fixed aft of the vertical stabilizer for yaw control.

Fuselage

The fuselage was constructed with a panel of aluminum honeycomb, to which balsa stringers and basswood bulkheads are fixed to provide the overall shape. In addition, the main landing gear is bolted onto the aluminum honeycomb. The wings fix onto the fuselage with threaded bolts, and are secured to the fuselage with small nuts. The remainder of the length of these bolts is used to secure the steel payload plates in the precise location of the airplane CG. Balsa stringers taper to the back tip, where the horizontal and vertical stabilizers are embedded into the fuselage structure. A balsa wedge is fixed to these stringers to serve as a connection point for the rear landing gear. The final fuselage shape resembles a symmetrical NACA 000012 airfoil.

Landing Gear

A controllable taildragger landing gear is installed for the rolling and maneuvering of the airplane on the ground.

Propulsion

The aircraft propulsion system includes a Magnum XLS-61A with a 14X4 propeller.

Center of Gravity

The results of physical testing show that the airplane is balanced at a CG location of 2.64 inches from the wing leading edge.

3. CALCULATIONS

3.1. PERFORMANCE

Performance was estimated through determining 3D drag effects and the payload capacity of the system.

3.1.1. 3D Drag Analysis

The 3D drag polar on an airplane can be approximated using Equation 1 [1].

$$C_D = C_{D_{min}} + K' {C_L}^2 + K''\left(C_L - C_{L_{min}}\right)^2 \quad (1)$$

In this equation, $C_{D_{min}}$ is a summation of the pressure and skin friction drag contributions from all airplane components, $K'$is the inviscid induced drag factor, C_L is the coefficient of lift at a given angle of attack, $K''$is the viscous induced drag factor, and $C_{L_{min}}$ minimum coefficient of lift.

$C_{D_{min}}$ is found by summing the contributions of each component, as calculated with Equation 2 [1].

$$C_{D_{min}} = \frac{FF \times C_f \times S_{wetted}}{S_{planform}} \quad (2)$$

In Equation 2, FF is the form factor, C_f is the skin friction coefficient, S_{wetted} is the wetted surface area, and $S_{planform}$ describes the planform area of the components. Table 4 shows these values computed at an anticipated level flight velocity of 40 feet per second. Also shown are the piece-wise 3D drag contributions of each aircraft component to the overall $C_{D_{min}}$.

Table 4: 3D drag contributions of components

Component	FF	Cf	Swetted (ft²)	Splanform (ft²)	CDmin
Wing	2.33	0.0026	15.03	7.17	0.013
Fuselage	1.44	0.0047	4.44	1.24	0.019
Horizontal Stabilizer	2.31	0.0040	2.86	1.38	0.016
Vertical Stabilizer	2.31	0.0032	2.30	1.09	0.025
Landing Gear	-	-	-	-	0.004
TOTAL					0.076

Then, the inviscid induced drag factor K' is calculated with Equation 3 [1].

$$K' = \frac{1}{\pi ARe} \tag{3}$$

In Equation 3, AR represents the wing aspect ratio and e is the wingspan efficiency. K', AR, and e were calculated to be 0.047, 7.17, and 0.935, respectively.

$C_{L_{min}}$ was determined as the point of lowest C_D from the drag polar shown on the left side of Figure 10. Then, the viscous induced drag factor K'' is determined as the slope of the nearly linear relation shown on the right side of Figure 10.

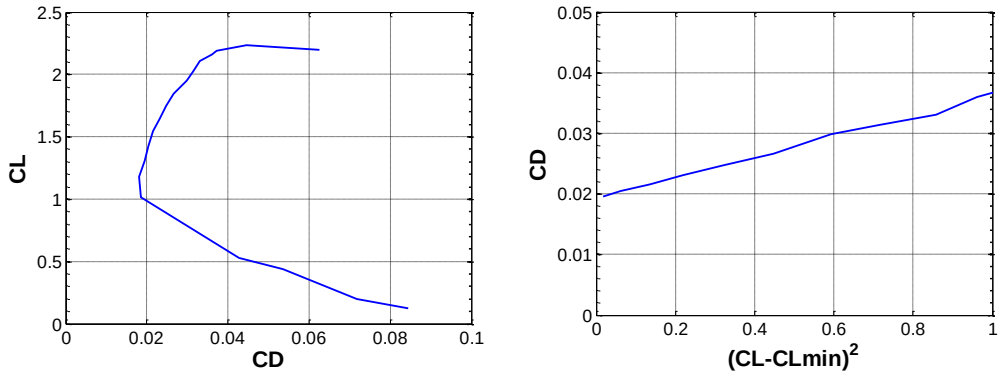

Figure 10: S1223 airfoil drag polar curve (left) and viscous induced drag factor estimation (right)

$C_{L_{min}}$ is computed as 1.1221 at a Reynolds number of 200,000 for the wing and K'' is found to equal .1715. Finally, these values can be substituted back into Equation 1 to obtain the airplane's 3D drag coefficient for all airfoil lift coefficients. Figure 11 shows this relationship and the lift to drag ratio.

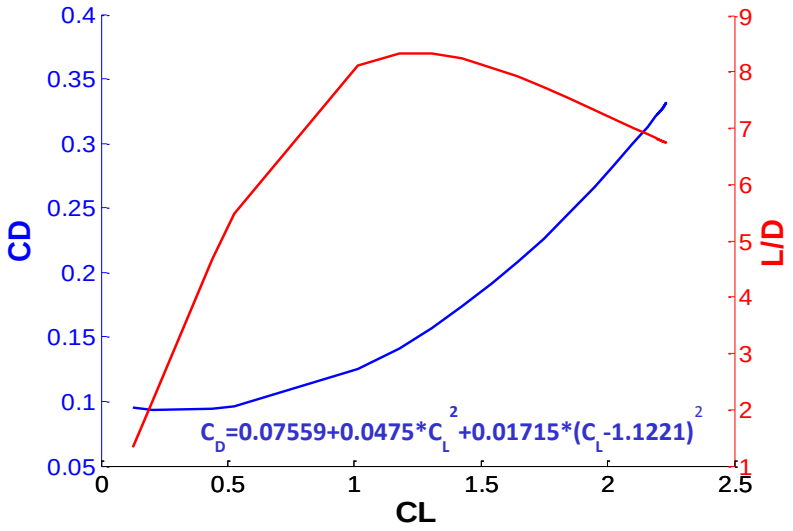

Figure 11: CD as a function of CL and lift to drag ratio for the airplane

Figure 11 was used to select the optimum angle of attack of 0.75 degrees, corresponding to a lift coefficient of about 1.18, drag coefficient of 0.14, and lift to drag ratio of 8.32. In addition, the equation shown is used to determine the total resulting 3D drag for the airplane traveling in one direction at 40 feet per second.

3.1.2. Performance Prediction

If an aircraft can generate enough lift to elevate off the ground, it can be considered suitable to maintain level flight. This concept is used as a basis for making payload predictions. A reasonable method for estimating the distance required for an aircraft to achieve lift-off is shown in Equation 4 below [5].

$$S_{LO} = \frac{1.44W^2}{g\rho_\infty S C_{L_{max}}\{T-[D+\mu_r(W-L)]_{ave}\}} \quad (4)$$

In Equation 4, s_{LO} is the liftoff distance, W is the aircraft weight, g is the force of gravity, ρ_∞ is the ambient air density, S is the wing planform area, $C_{L_{max}}$ is the maximum lift coefficient, T is the thrust provided by the engine, D is the total aircraft drag, μ_r is the coefficient of rolling friction, and L is the lift required for takeoff.

In these calculations, a liftoff distance of 195feet was selected to provide a flexible window for takeoff within the allotted 200 foot distance as provided by requirement R1. The remaining variables, except for air density and weight, were assigned constant values determined by analyses discussed above. In particular, the thrust value assigned was the static thrust determined from physical testing. Drag was determined from the drag coefficient quantified in the 3D Drag Analysis section above. Rearranging Equation 4 to the form of Equation 5 allows the weight to be determined as a function of air density in calculations. Equation 5 is shown below.

$$W = \sqrt{\frac{s_{LO} g \rho_{\infty} S C_{L_{max}} \{T - [D + \mu_r (W - L)]_{ave}\}}{1.44}} \tag{5}$$

Here, the weight term within the square root necessitates the implementation of a numerical MATLAB script which inputs an initial weight guess and reiterates until the weight is determined within a desired level of accuracy. This process is repeated for a sweep of air densities calculated directly as a function of elevation. The result is a linear payload prediction graph, attached to this document as Appendix B.

3.2. STABILITY AND CONTROL

Longitudinal Stability

Longitudinal stability is primarily achieved through the adequate sizing of the horizontal stabilizer and the proper placement of the aircraft center of gravity. An important measure of the tail effectiveness is the horizontal tail volume coefficient [7], shown in Equation 6.

$$V_H = \frac{S_H l_H}{Sc} \tag{6}$$

In Equation 6, S_H is the horizontal stabilizer planform area, l_H is the horizontal stabilizer moment arm, S is the wing planform, and c is the wing chord. A stable aircraft typically has a V_H value between 0.3 and 0.6 [7]. Thus, the horizontal stabilizer was dimensioned in order to achieve a tail volume coefficient of 0.55 in support of objective O3.

Another criterion for longitudinal stability is that the CG of the aircraft should sit very near to the aerodynamic center of the wing. For typical airfoils, this point is very close to 25% of the mean wing chord. However, for a highly cambered airfoil such as the S1223, this point is shifted a bit forward. Therefore, in support of objective O3, the aircraft was constructed so that the CG was at 22% of the mean wing chord.

Spiral Stability

Spiral stability is most often achieved through the implementation of a dihedral angle in the wings [7]. Following flight test results which demonstrated a need for more stability in this direction, a dihedral of angle of 3° was implemented into the design in order to support objective O3.

Aileron Sizing

The ability for an aircraft to effectively maintain roll control, for the support of objective O4, is highly dependent on the aileron size. For maximum efficiency, the ailerons must be properly dimensioned with respect to the wing planform. Parameters used for proper sizing include the aileron planform S_a, aileron chord to span ratio C_a/b_a, aileron deflection $\pm\delta_{A\max}$, and distance from the inner edge to the wing center b_{ai}. Figure 12 below shows a schematic of these dimensions.

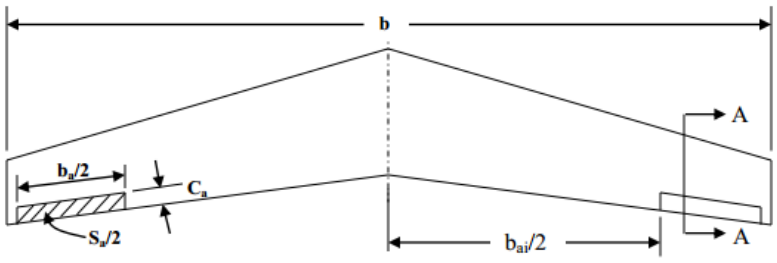

Figure 12: Aileron Dimensioning

Typically, proper aileron dimensioning adhere to the following ranges, $\frac{S_a}{S} = 0.5 - 0.1$, $\frac{b_a}{b} = 0.2 - 0.3$, $\frac{C_a}{C} = 0.15 - 0.25$, $\frac{ba_i}{b} = 0.6 - 0.8$, and $\delta_{Amax} = \pm 30°$ [8]. Specific aileron dimensioning for the "Tomahawk" can be seen in Appendix B.

Servo Sizing

The proper servo must be selected to ensure the function of all control surfaces in support of objective O4. Each surface experiences a different amount of force, so each servo needs to be sized according to its respective control surface. Torque calculations are dependent on the control surface chord C, velocity V, control surface length L, maximum control surface deflection S_1, and max servo deflection S_2 [9]. Equation 7 outlines the appropriate torque calculations for servo sizing.

$$T(oz - in) = 8.56x10^{-6}\left(\frac{C^2V^2Lsin(S_1)}{\tan(S_2)}\right) \quad (7)$$

Equation 7 generates torque values for the ailerons, elevator, and rudder as 31.413 oz-in, 28.721 oz-in, and 36.698 oz-in, respectively.

3.3. STRUCTURAL ANALYSIS

3.3.1. Landing Gear Finite Element Analysis

Using the COSMOS finite element analysis software, a 2D truss structure was modeled for the main landing gear system, as shown in Figure 13.

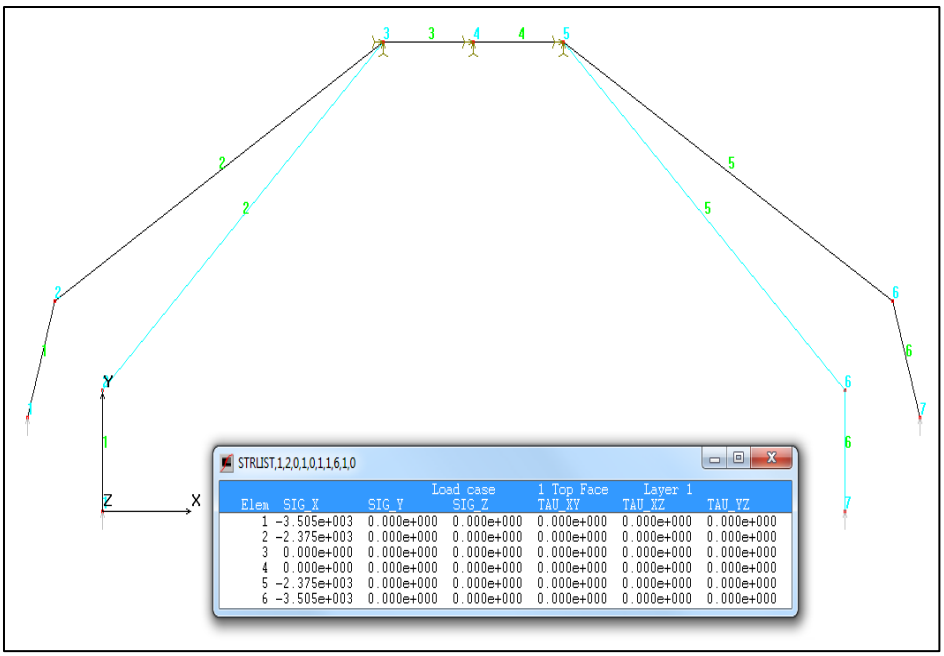

Figure 13: 2D FEA analysis of main landing gear

The maximum force of impact was found to be 876.3 pounds acting on each arm with a 20° angle of incidence. The assumption that nodes three four and five are perfectly fixed to the fuselage was made so that no forces and or stresses will be acting on those members. Based upon the material properties of the aluminum bar, the stresses acting on each of the elements were found, as shown in Table 5.

Table 5: Bending stress on main landing gear due to impact

Element	Stress (ksi)
1	-3.505
2	-2.375
3	0
4	0
5	-2.375
6	-3.505

With a yield strength of 40 ksi for the aluminum landing gear, a minimum factor of safety of 11.4 was found for the given stresses. This analysis supports the fulfillment of objective O5, as it demonstrates the ability of the main landing gear to predictably withstand the maximum possible landing impact.

3.3.2. Wing Spar Analysis

Wing spars were designed to provide the adequate bending strength to the wings while also minimizing the associated weight, in support of design objectives O5 and O6. The spar selection process began with shear force and bending moment analysis, as shown in Figure 14.

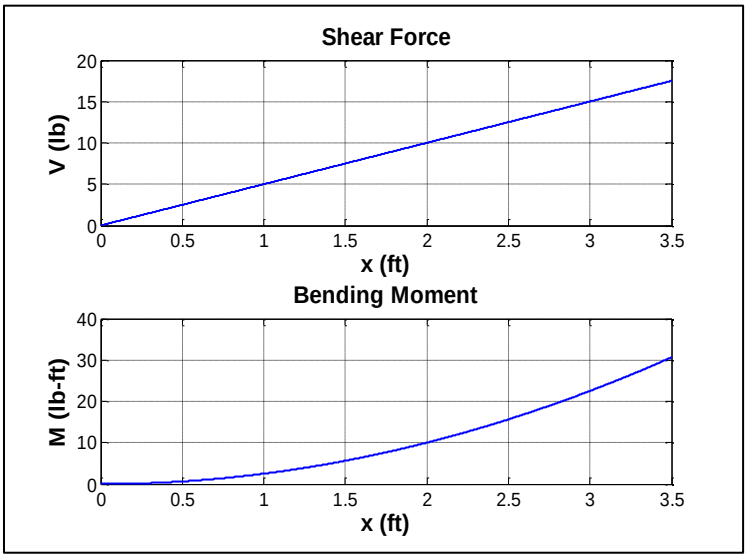

Figure 14: Wing spar shear force and bending moment analysis

The basis for this analysis was the modeling of half a wing as a cantilever beam experiencing a uniformly distributed load. This load totaled to 35 pounds of lift, a generous expected value for total lift. To save weight, the front and rear spars were sized to a narrow factor of safety of 1.5 based on an applied bending moment of 20 pound-feet. This is possible because the most significant bending forces only occur in the middle 1.5 feet of the wing, as seen in the lower portion of Figure 14. To support the wings under the strong bending occurring at the middle of the wings, a center spar was added which spanned only the central 1.5 feet of the wing. This careful analysis resulted in the selection of spars that were minimally sized, yet supplied the necessary structural support.

3.4. COMPETITIVE SCORING ANALYSIS

The mission strategy for the competition was devised through a thorough study of the scoring system as laid out by SAE. A MATLAB script was written to determine the optimal blend of raw weight

scores and prediction bonus points. Figure 15 shows a curve of theoretical scores, along with possible scores as determined by the payload weight increments the system physically allows. This curve showed the team that a payload of 14 pounds would give a better score than the next possible payload of 17.5 pounds. It also shows that 21 pounds would give a better score.

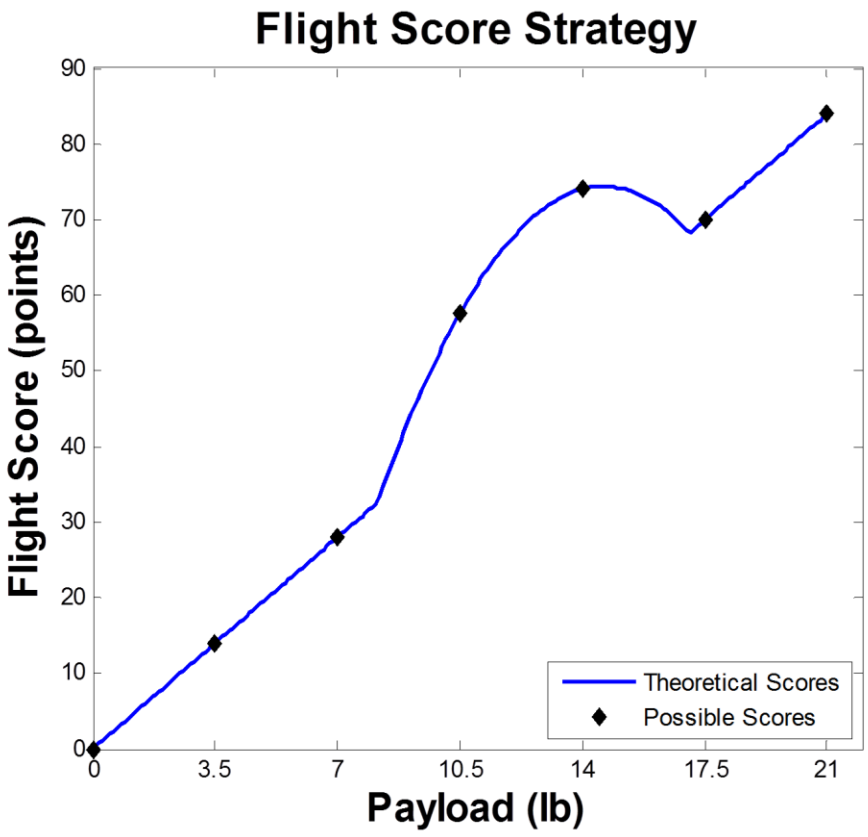

Figure 15: Flight score strategy

This analysis led the team to an optimal mission strategy. The first round will consist of an unloaded flight for an empty flight bonus of 10 points. The second round will consist of a 14 pound payload which will give the optimal combination of raw weight and prediction bonus points. In all other rounds, the plane will carry 7 pounds of payload, which is the amount of weight at which the aircraft flies best according to the pilot. This will allow the team to maintain a high reliability score, which determines a multiplier of the best achieved flight score. A "max-out" weight of 21 pounds will be sought if the pilot considers it to be possible.

4. INNOVATIONS

4.1. ADDITIVE MANUFACTURING

The most unique element of this team's design is the use of additive manufacturing with ABS polymer for rib and cowling construction. There are several limitations to the use of balsa wood for rib construction, mainly pertaining to its structural weakness which leads to diminished workability. This is especially significant when the airfoil used has very thin sections. With the selection of the S1223 airfoil for aerodynamic purposes, this design team was especially concerned about fabricating the very thin trailing portions of our ribs out of balsa. Additionally, the implementation of very small features such as the thin balsa support inlets seen in our ABS airfoils requires a level of precision that would be extremely difficult to achieve if we had been hand-tooling balsa ribs. Figure 16 displays the side view of the complex rib shape.

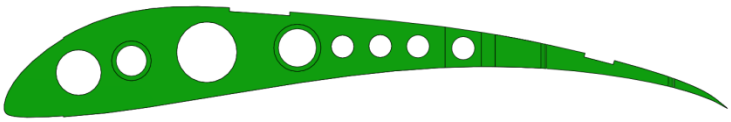

Figure 16: ABS rib profile

While the team acknowledges a weight disadvantage of using ABS polymer over balsa, we believe that the smooth curvature of the wing more than compensates for the extra weight. The aerodynamic performance of our aircraft will undoubtedly benefit from the streamlined surfaces created by the uniform rib sections.

5. COMPETITION RESULTS

In the Aero Design West 2013 competition, the airplane designed by The Wright Stuff achieved a 14th place finish overall out of 37 teams. The design report submitted a month ahead of the competition received a score of 36.95 out of 50. This was the 24th ranked report. On the first day of

competition, the team passed the technical inspection with no penalties. In addition, the team delivered the 1st place oral presentation, earning a score of 47.33 out of 50.

The next two days consisted of six flight rounds, in which the mission strategy was completed almost perfectly. The first flight of the competition was successfully completed for an empty weight bonus of 10 points. The next two flights were plagued by engine failures, leading to catastrophic crashes. Nevertheless, the team was able to successfully troubleshoot any failures and rebuild the airplane before the last round of the day. The aircraft carried 7 pounds of payload on the fourth flight of the day. On the final day of competition, the aircraft successfully carried its target weight of 13.8 pounds, earning a weight prediction bonus of 18.56 in addition to the raw weight score of 55.2. The ability of the team members to efficiently identify failure modes and rebuild successfully was instrumental in the team's success at competition.

6. LESSONS LEARNED

Numerous lessons were learned throughout the design, build, and competition phases of this project. The team believes that the following lessons were the most important:

- Save more time for the preliminary design and build processes by de-emphasizing conceptual perfection
- In order to leave as much time as possible for flight testing and rebuilding, build the first prototype as soon as possible
- Consider longitudinal stability and center of gravity location before starting to build the airplane
- Fully utilize the maximum aircraft weight and dimensions allowed by SAE

7. CONCLUSION

The Wright Stuff design team of NAU has conducted a complete conceptual design, performed thorough engineering analysis, and completed the construction of a final design that met the requirements laid out by the Society of Automotive Engineers for the Aero Design West competition.

With a low weight of only 11.4 pounds and a smooth, streamlined body that could only be achieved with the best in computer-aided manufacturing, the “Tomahawk” successfully accomplished its stated goals at competition. The use of additive manufacturing techniques was instrumental to the success of the team by allowing the construction of precise shapes with optimal aerodynamic characteristics. The team earned a 14th place finish out of 37 teams at the 2013 Aero Design West competition.

8. REFERENCES

[1] Nicolai, Leland. *Estimating R/C Model Aerodynamics and Performance*. Tech. N.p.: n.p., 2009. Print.

[2] Drela, Mark. "XFOIL 6.97." *XFOIL Subsonic Airfoil Development System*. Ed. Harold Youngren. N.p., Apr. 2008. Web. 04 Mar. 2013.

[3] Anderson, John. *Fundamentals of Aerodynamics*. 5th ed. New York: McGraw-Hill, 2011. Print.

[4] Raymer, Daniel P. *Aircraft Design: A Conceptual Approach*. 3rd ed. Reston, VA: American Institute of Aeronautics and Astronautics, 1999. Print.

[5] Anderson, John. *Introduction to Flight*. 2nd ed. New York: McGraw-Hill, 1985. Print.

[6] "Pilot's Handbook of Aeronautical Knowledge." *Pilot's Handbook of Aeronautical Knowledge Chapter 1*. N.p., n.d. Web. 04 Mar. 2013

[7] "Basic Aircraft Design Rules." *Http://ocw.mit.edu/courses/aeronautics-and-astronautics/16-01-unified-engineering-i-ii-iii-iv-fall-2005-spring-2006/systems-labs-06/spl8.pdf*. N.p., 6 Apr. 2006. Web. Feb. 2013.

[8] "Aircraft Design: A Systems Engineering Approach." *Wiley:*. N.p., n.d. Web. 04 Mar. 2013.

[9] Gadd, Chuck. "Servo Torque Calculator." *Calculate Required Servo Torque*. N.p., n.d. Web. 04 Mar. 2013.

Pertinent Information					
Wingspan	Chord	Tail Span	Center of Gravity	Empty Weight	Motor
89.88"	12.00"	36.00"	14.61"	9.00 lb	Magnum XLS 61A

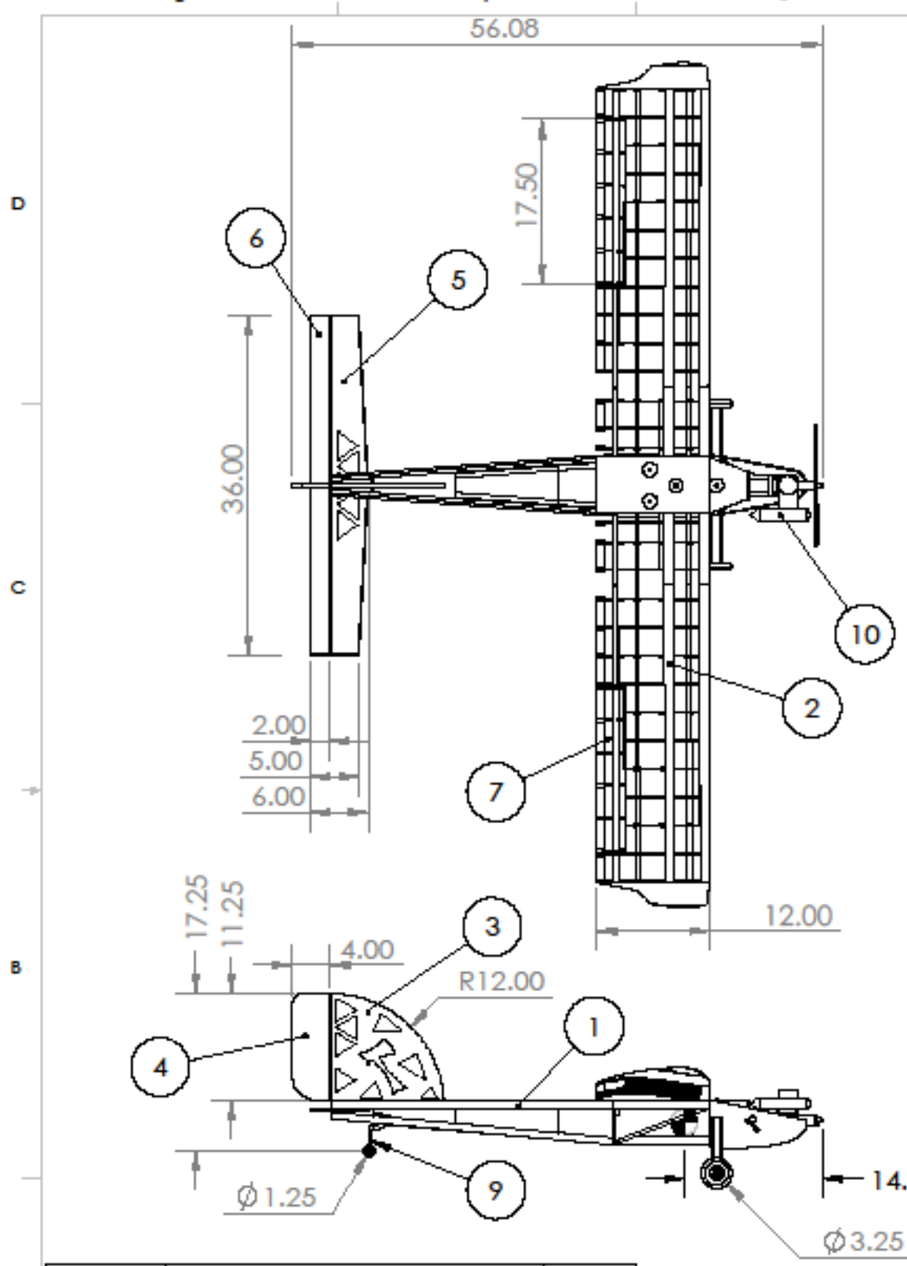

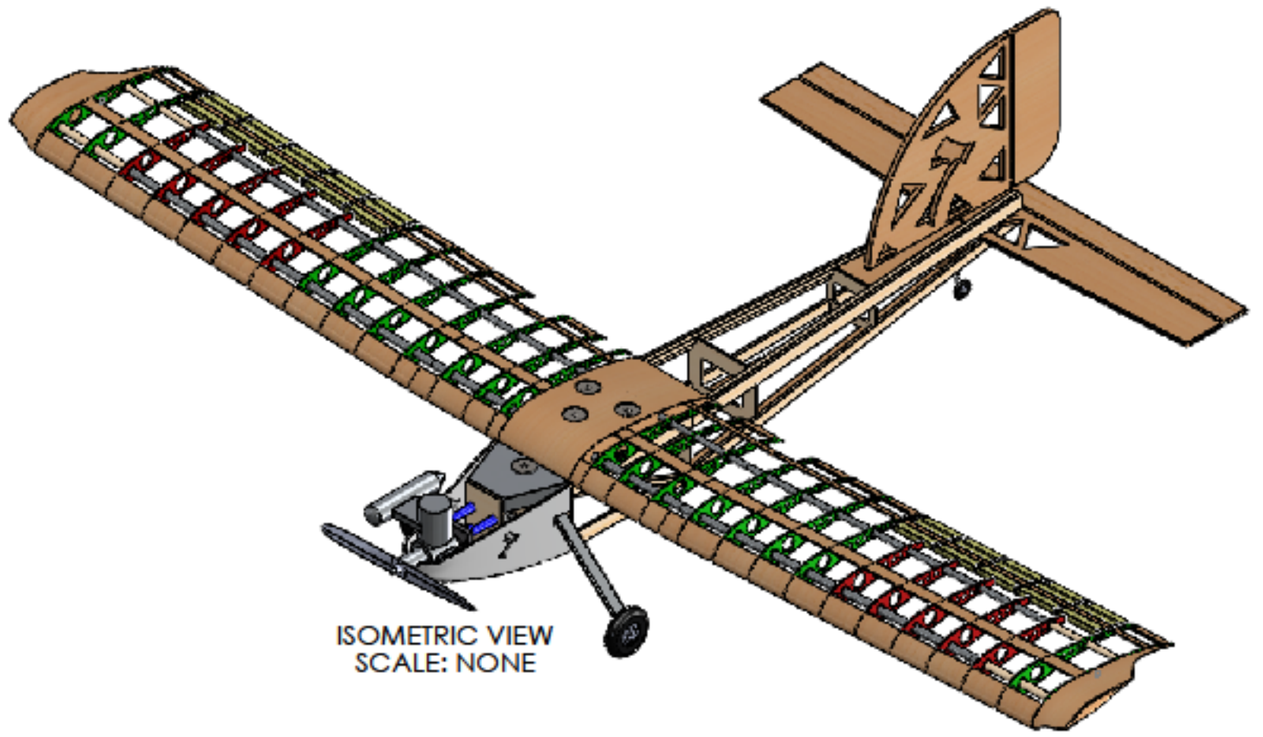

ISOMETRIC VIEW
SCALE: NONE

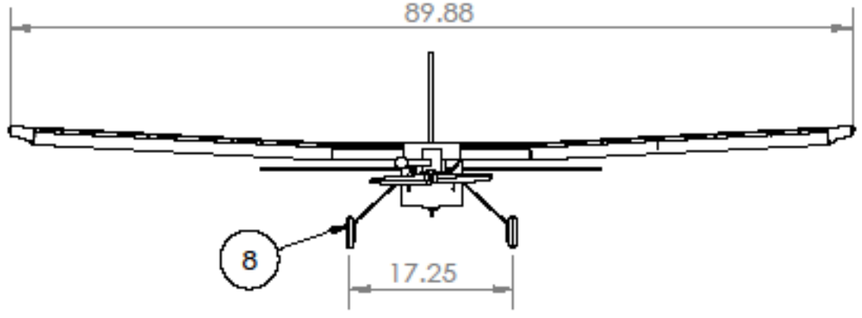

ITEM NO.	PART NUMBER	QTY.
1	Fuselage	1
2	Wing	1
3	Vertical Stabilizer	1
7	Rudder	1
5	Horizontal Stabilizer	1
6	Elevator	1
7	Aileron	2
8	Landing Gear Assy - Front	1
9	Landing Gear Assy - Rear	1
10	Engine Assembly	1

NEXT ASSY | USED ON

APPLICATION

UNLESS OTHERWISE SPECIFIED:

DIMENSIONS ARE IN INCHES
TOLERANCES: 0.25
FRACTIONAL ± 0.25
ANGULAR: MACH ± BEND ±
TWO PLACE DECIMAL ±
THREE PLACE DECIMAL ±

INTERPRET GEOMETRIC TOLERANCING PER:

MATERIAL: VARIES

FINISH: VARIES

DO NOT SCALE DRAWING

	NAME	DATE
DRAWN	AAL	3/1/13
CHECKED	BRP	3/1/13
ENG APPR.		
MFG APPR.		
Q.A.		

COMMENTS:

Appendix A

TITLE:

NORTHERN ARIZONA UNIVERSITY
THE WRIGHT STUFF
TEAM 022

SIZE	DWG. NO.	REV
B	Tomahawk	3

SCALE - 1:16 | WEIGHT: 9 lbs | SHEET 1 OF 1

APPENDIX B: PERFORMANCE PREDICTION

The Wright Stuff from Northern Arizona University